

Plasma synthesized polysilanes — organic nanostructural materials

F. Schauer^{a,*}, P. Horváth^b

^a Faculty of Technology, Polymer Centre, T. Bata University in Zlin, T.G.Masaryk sq. 272 CZ, 762 72 Zlin, Czech Republic

^b Faculty of Chemistry, Technical University of Brno, 612 00 Brno, Czech Republic

Received 3 January 2003; accepted 14 July 2003

Abstract

The search for new organic materials with applicational potential has recently led to heterogeneous nanostructural systems in general, and plasma polymers in particular. The reasons for this are twofold — first, we can easily prepare polymers that are difficult to synthesize by other means and second, we can produce a set of materials with properties and structure changing in a wide range. This study reports the results achieved in plasma polymerization of polysilylanes in radio-frequency and microwave discharges. Langmuir probes, in situ mass spectrometry and cryogenic sampling and chromatography characterized the plasma and polymerization conditions, and the plasma synthesized polysilane films by the methods of absorption and infrared spectroscopy, desorption spectroscopy and steady state and transient fluorescence. The set of conditions were established for the optimum plasma polymerization, structure and microphysical properties of the films. As the main applicational area of the plasma polysilanes was luminescence, the stability was of prime interest.

© 2003 Elsevier B.V. All rights reserved.

Keywords: Plasma polymerization; Polysilane films; Fluorescence

1. Introduction

In the late 80th the cumulative and review papers on high molecular weight polysilylenes published by Miller and Michl [1] and Harrah and Zeigler [2] marked the start of an extensive interest and complex elucidation of optical and electronic properties of this new class of organic silicon based materials [3–5]. This development was a part of a more general study of silicon based materials as summarized in excellent review papers by Matsumoto [6] and Brus [7], and this development has been lasting till present days.

It has been obvious from the very start and still is that high molecular weight polysilylenes possess suitable properties for luminescence and electro optic applications in general [8] for their high transport [9], photoconductivity [10], non-linear optical properties [11], luminescence in ultraviolet (UV), visible [12] and also white light. On the other hand the liability to UV

degradation led to the search for chemical modification by fullerene doping [13] and new materials with increased dimensionality (2D and 3D compared to 1D polysilylene) [14,15]. Suzuki et al. [16] used the UV laser ablation of polymethylphenylsilylene and Watanabe et al. [17] used 266 nm laser for chemical vapour deposition (CVD) polymerization of dichloromethylphenylsilylene.

The plasma polymerization is one of the prospective methods of preparation of silicon-based organic materials. The plasma polymerization method is known as the method by which polymerised materials are easily obtained even if the monomer does not have functional groups for polymerization [18]. In order to control the polymer structure mesh screen [19] and low power plasma polymerization [20] were used. Recently, Nagai et al. [21] used inductively coupled radio-frequency (RF) and monomers were phenylsilylene and methylphenylsilylene, dimethylphenylsilylene and trimethylphenylsilylene. They found the change of the structure from 1D polysilylene to 3D carbidic structure with the increased power of the RF discharge. Wrobel et al. [22] used RF remote hydrogen plasma CVD and tetrakis trimethylsilylsilane as a monomer and determined the influence of

* Corresponding author. Tel.: +420-57-603-1320; fax: +420-57-603-1444.

E-mail address: fschauer@ft.utb.cz (F. Schauer).

the important process parameter — substrate temperature — on the dimensionality of the produced material. Wrobel et al. in [23] used microwave (MW) remote hydrogen plasma, where UV and particles bombardment damage was limited. They used hexamethyldisilane and trimethylsilylene as a monomer and found, using cryogenic sampling and gas chromatography, the important growth step by Si–CH₂–Si bridging.

The present paper summarizes the results achieved in our laboratory [24] in preparing the organo silicon plasma polymer films by plasma polymerization both by radio-frequency plasma enhanced chemical vapour deposition (RF PE CVD) and by the remote microwave electron-cyclotron-resonance plasma enhanced chemical vapour deposition (MW ECR PE CVD). In both cases of plasma polymerised films we will use the name plasma polymers, or plasma PMPHSi. It is necessary to point out that a plasma polymerised material is not a unique one, as plasma materials may constitute a set of materials with properties changing in a broad interval, strongly depending on the plasma parameters.

The main goal of the present study was to examine the resulting plasma nanostructural organosilicon material with respect to possible (electro)luminescence applications and increased stability to both UV radiation and injection of charge-carriers from the contacts.

2. Experimental

2.1. Plasma polymerization in general

We are interested in plasma polymerization of organic silicon based materials which cannot withstand temperatures exceeding a few hundreds of Kelvin, so we cannot use the thermally equilibrium plasma. That is the reason for the interest in the non-equilibrium plasma, in which the ionization proceeds by ‘hot’ electrons accelerated by electric field. In the glow discharge plasmas at a low pressure the neutral gas and ions are at low effective temperature less than 10³ K, while electrons can gain high energy (equivalent to 10⁴–10⁵ K in thermal equilibrium system) that enables many reactions to take place. To understand the plasma deposition processes, it is necessary to know also the energy of species bombarding the surfaces adjacent to plasma. In order to achieve reproducible results of plasma polymerization all these conditions must be considered and controlled.

For the preparation of plasma polysilylenes we used RF and MW plasma techniques. The two techniques of plasma polymerization are different in many aspects: the mechanism of excitation of monomer, presence or absence of the energy-carrier carrier gas, the electron temperature, plasma density and the intensity of ion bombardment.

2.2. Radio-frequency plasma enhanced CVD (RF PE CVD)

The first method for the plasma polysilylenes preparation was RF PE CVD method, in the reactor based on the 13.56 MHz RF glow discharge apparatus with the capacitively coupled plasma (Fig. 1). After pumping down, the reaction chamber was flushed for 30 min by hydrogen and heated to ca. 150 °C. During deposition the RF plasma excited the mixture of hydrogen and monomer vapours. Both gases were introduced directly into the plasma discharge. Adjusting the temperature of the monomer container at about 30–50 °C controlled the monomer partial pressure. We choose the conditions for the homogenous plasma polymer film growing with reasonable growth rate by the power of the discharge and monomer and hydrogen partial pressures ratio together with the total pressure.

The addition of hydrogen is essential to avoid the powder formation in the discharge volume as well as for appropriate film quality caused by the hydrogen etching of the growing surface. The deposition took usually about 40 min. After deposition samples were kept for another 30 min at 100 °C in hydrogen atmosphere to minimise contamination and structural relaxation and then cooled to the room temperature. The high electron temperature in RF plasma (in excess of 10 eV — see Fig. 3) provides sufficient energy for the cleavage of all in monomer (methylphenylsilane and dichloromethylphenylsilane) present bonds — Si–Si 2.2 eV, Si–C 3.2 eV, Si–H 3.47 eV, C–C 3.69, Si–Cl 3.8 eV [16].

2.3. Microwave frequency plasma enhanced CVD ((MW) ECR PE CVD)

Power from magnetron Hitachi 2M107A (with a frequency of 2.45 GHz) was introduced into the quartz glass discharge chamber through a wave-guide — Fig.

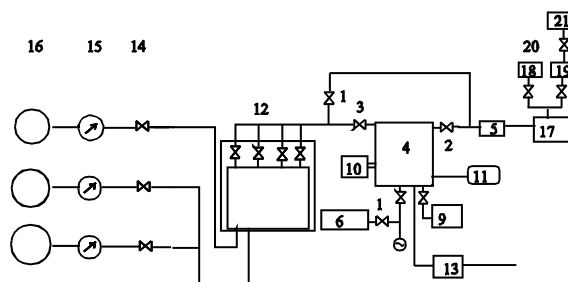


Fig. 1. Scheme of RF PE CVD technology (1, 2, and 3) vacuum valves; (4) reaction chamber; (5) Pirani pressure gauge; (6) titan ion pump; (9) ‘baratron’ capacity pressure meter; (10) RF power supply generator; (11) monomer supply bin; (12) control gas flow valves gauge; (13) electronically controlled gas flow meter; (14) reduction valves; (15) manometers; (16) gas bombs; (17) Roots rotary pump; (18, 19) rotary oil pumps; (20) vacuum valve; (21) exhaust gasses combustion chamber.

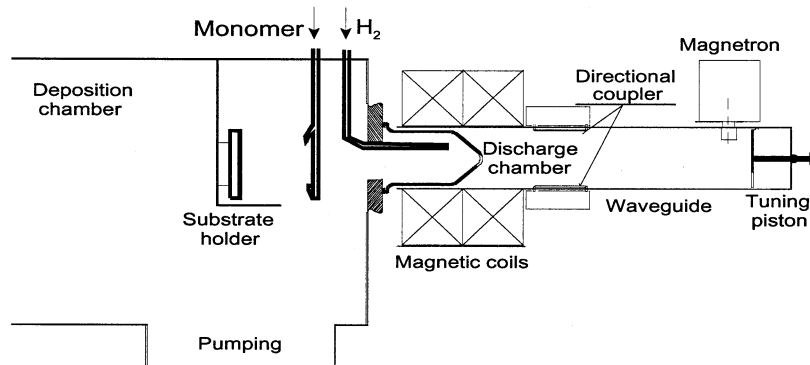


Fig. 2. ECR MW PE CVD processing chamber.

2. The hydrogen as a carrier gas was ionised and excited by MW power in a reaction chamber. Two magnetic coils surround the discharge chamber forming the magnetic field and establish the ECR condition. Under these conditions the MW-driving field required to ignite and sustain plasma is minimized. The monomer is fed into a processing chamber where it collides with excited carrier gas emerging from discharge chamber and reacts onto the substrate forming a thin film. The procedure for the synthesis of the polymer films were as follows: the system was evacuated to the base pressure of 2×10^{-3} Pa and then hydrogen as a carrier gas was introduced into a processing chamber and 180 W of MW power for 30 min served to eliminate contamination of reactor and to stabilise deposition conditions generated the hydrogen plasma. Then the vapour of monomer was introduced into the reactor. The deposition pressure was typically 0.15 Pa, the flow rate of hydrogen was 30 sccm. After the deposition hydrogen plasma alone was kept for some time to minimise the contamination of the polymer film. In remote plasma conditions the excitation mechanism are more straightforward compared to RF plasma. As we used hydrogen as the carrier and excitation gas in remote plasma regime, the only excitation long lived species were $H_2(C3\Pi_u)$ at 11.75 eV.

2.4. Other experimental techniques

Throughout this study methylphenylsilane and dichloromethylphenylsilane (Fluka) monomers were used for both RF PE CVD and MW ECR PE CVD. Hydrogen of purity 99.999%, was used. Plasma conditions were monitored by several techniques. Besides the standard techniques as temperature and partial pressure measurements, we used the techniques of Langmuir probes measurements for electron temperatures and ion concentrations, in situ optical spectroscopy and mass spectrometry of ambient gasses. For the study of the film growth mechanisms we used the cryogenic sampling technique combined with gas chromatograph and mass

spectrometer with cross beam ioniser with adjustable electron energy in the interval 5–70 eV (GC MS chromatograph TRIO 1000, FISON INSTRUMENTS (USA) with the column DB-5MSITD). For the UV–vis absorption, infrared (IR) absorption and photoluminescence (PL) measurements the HITACHI U300, NICOLET 400 FTIR and IR microscope the FT-IR microscope CONTINUUM NICOLET and fluorimeters Aminco–Bowman Series 2 and Perkin–Elmer LS 55 with Xe lamp were used. For the desorption measurements the apparatus equipped with LEYBOLD 200 mass spectrometer was built. For degradation experiments the 266 and 355 nm wavelengths of the NdYAG laser CONTINUUM MINILITE II (Electro-Optics) and the CCD camera Oriel, model DB 401-UV, for scanning the fluorescence spectra were used.

For the comparison purposes we used the poly(methyl-phenyl silylene) prepared by Wurtz coupling (details of preparation see [4]) and deposited from toluene solution by spin coating on quartz glass (for optical transition measurements) or single crystal Si wafers (for PL, IR absorption and desorption studies). These films will be next named solution processed PMPHSi films compared to plasma prepared PMPHSi films.

3. Experimental

3.1. Basic characterization of plasma polymers

The main goal of our study was to find the basic conditions of the RF plasma for the suppressing the gas phase reactions and producing the optimum structure, for PL properties, of the nanostructural organosilicon films. The main process parameters were the hydrogen and monomer partial pressure giving the total gas pressure and the RF power. We found from electrical and PL measurements the optimum total gas pressure to be in a range 80–90 Pa with the hydrogen partial pressure 60 Pa and the monomer partial pressure in a

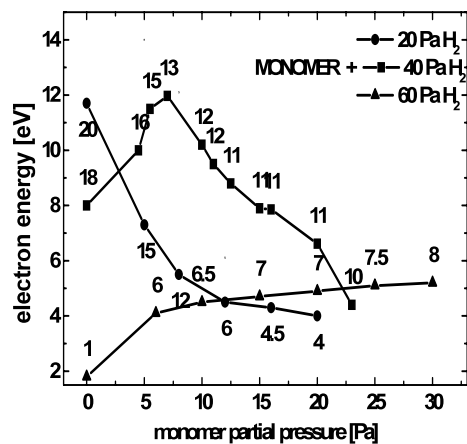


Fig. 3. The electron temperature as the function of the monomer partial pressure in RF discharge parametric in the hydrogen partial pressure — the numbers at the points denote the plasma potential in V.

small range 20–30 Pa, where the plasma potential and electron energy tends to be minimized (see Fig. 3). It is interesting that the probe measurements in Fig. 3 gave for the hydrogen partial pressure 60 Pa both electron energy and plasma potential nearly independent on monomer pressure compared to dependences for the hydrogen partial pressure 20 and 40 Pa. The PL spectra as well as their integral intensities depend also on the hydrogen and monomer partial pressures. For example the approximate values of integral PL intensities of plasma prepared PMPHSi samples are shown in the Fig. 4. PL intensity exhibits maximum for about 30–50% monomer to hydrogen partial pressure ratio.

The plasma films were smooth in several tens of nanometer scale as visible in Fig. 5 a where roughness of the RF plasma film is plotted. The adherence to both silica glass and Si single crystals were excellent, the mechanical hardness of the film was also very good [25],

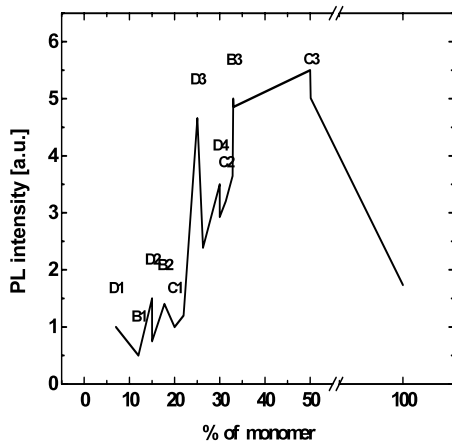


Fig. 4. The cumulative dependence of integrated PL intensity on the monomer to hydrogen partial pressures ratio, the letters are samples labels used in Fig. 7.

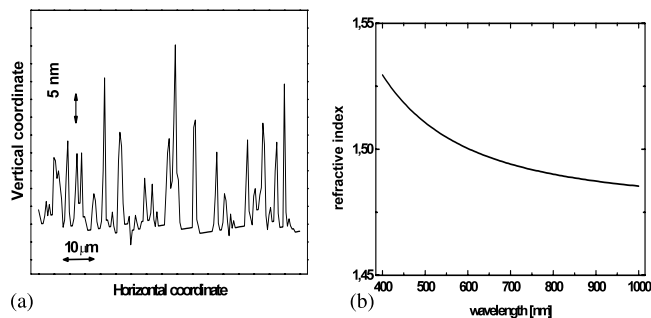


Fig. 5. The surface roughness of the RF plasma polymer (a) and its dispersion dependence of the refractive index (b).

the index of refraction showed only small dispersion, Fig. 5b.

The additional information on the composition and structure of the solid films of plasma polysilenes comes from the thermal desorption spectroscopy [26]. On heating the sample with linear temperature ramp with the fixed slope the desorption of the chemical species may be observed. In Fig. 6 are typical spectra of RF plasma prepared PMPHSi. There are three desorbed species observed — the first in the temperature range 300–550 °C (and maximum at 470 °C) corresponding to phenyl group ($m/z^+ = 78$ and 77 — molecular mass/effective molecular charge), CH₃ in the range of temperature 300–650 °C (with maxima at 455 and 584 °C, originating from two environments for release of CH₃ species) and H (with maximum at about 600 °C).

Results of the desorption spectroscopy of the RF plasma films prepared with varying pressures of both monomer and hydrogen (samples of the series B, C and D) are in Fig. 7. The differences of the samples due to varying partial pressures of reaction gases are reflected very distinctly in thermal desorption spectra. We found experimentally, based on PL measurements, that the indicator of the nanostructural character (i.e. the existence of controlled 1D polysilylene islands embedded in 3D amorphous organo silicon network, exhibiting strong excitonic PL) is the highest possible temperature of all desorbed species, with minimum of

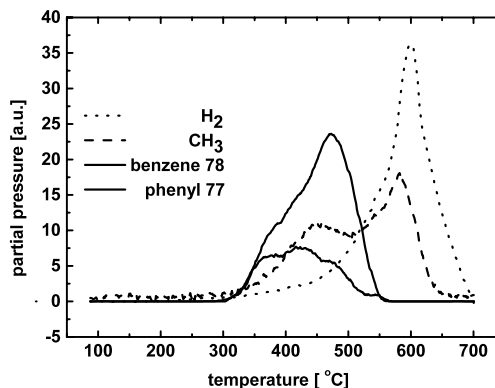


Fig. 6. Desorption spectra of RF plasma prepared PMPHSi.

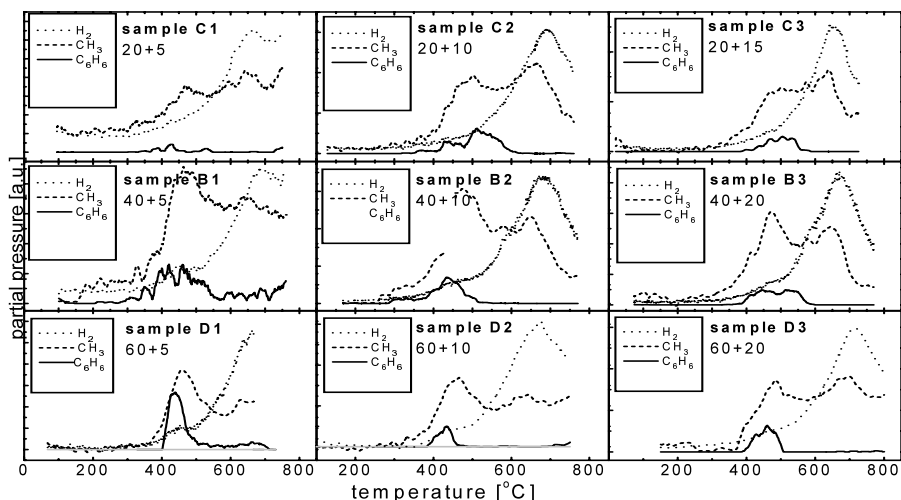


Fig. 7. Desorption spectra of plasma PMPHSi prepared with RF power 1.4 W cm^{-2} , substrate temperature $80 \text{ }^\circ\text{C}$, parametric in partial pressure of hydrogen and monomer.

phenyl peaks ($m/z^+ = 78$) in a thermal desorption spectrum. It is manifested on desorption spectra of a series D in Fig. 7 — on increasing the monomer partial pressure the peak of desorption curve for hydrogen shifts gradually from $660 \text{ }^\circ\text{C}$ (5 Pa) through $675 \text{ }^\circ\text{C}$ (10 Pa) to $720 \text{ }^\circ\text{C}$ (20 Pa), further increase of a monomer partial pressure leads to reduction of the hydrogen peak maximum below $690 \text{ }^\circ\text{C}$ and deterioration of both PL and mechanical properties of the films. The methyl desorption curves of series D exhibit similar features on increasing the partial pressure of monomer (see series D). Though the first peak position near $480 \text{ }^\circ\text{C}$ remains fixed, the second one moves from about $620 \text{ }^\circ\text{C}$ (5 Pa) to $700 \text{ }^\circ\text{C}$ (20 Pa). It is possible to conclude, on the basis of the desorption spectroscopy measurements, that there is an optimum monomer and hydrogen partial pressures for preserving the nanostructural character of RF plasma prepared organosilicon films. The deviations from these conditions result in the disappearance of the nanostructural effects in PL and deteriorated mechanical properties. The higher partial pressure of the monomer results in an intense powder formation in the plasma volume and a deteriorated quality of polymer films. On the other hand a polymer films prepared with less or no hydrogen partial pressure exhibit highly porous and disordered structure with the massive powder inclusions in the film.

The properties of plasma prepared PMPHSi, both in RF and MW discharges, were studied also by IR absorption spectroscopy and compared with the IR absorption spectra of solution processed PMPHSi (Fig. 8). The spectra prove the similarity of main vibrational modes of solution processed and plasma prepared films representing the basic building bonds of PMPHSi [27,28]: C–H asymmetrical stretching mode in CH_3 ($2950\text{--}2960 \text{ cm}^{-1}$), C–H symmetrical stretching mode in CH_3 ($2890\text{--}2910 \text{ cm}^{-1}$), Si–H stretching mode in Si–

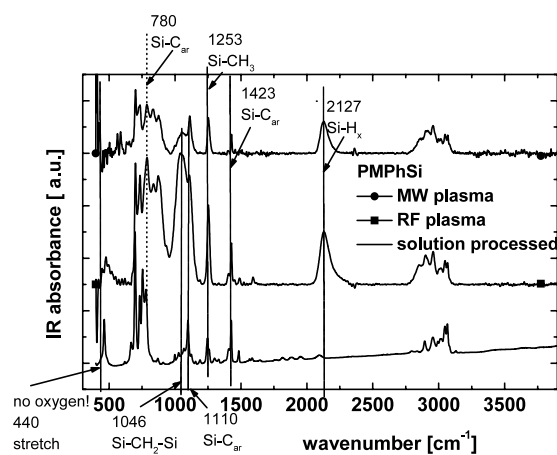


Fig. 8. Comparative IR absorption spectra of RF and MW plasma prepared and solution processed PMPHSi films.

H_x ($2100\text{--}2200 \text{ cm}^{-1}$), Si–C_{ali} symmetrical deformation in $\text{Si}(\text{CH}_3)_x$ ($1240\text{--}1260 \text{ cm}^{-1}$), Si–C_{ar} in Si–Ph (1120 and 1427 cm^{-1}), Si–C_{ali} wagging mode in Si–CH₂–Si ($1039\text{--}1050 \text{ cm}^{-1}$) and Si–O–Si bonds ($980\text{--}1046 \text{ cm}^{-1}$), Si–C carbidic stretching mode ($800\text{--}830 \text{ cm}^{-1}$) Si–O mode (470 cm^{-1}). Comparing the IR spectra of all three materials we can see that all vibrations present in solution processed PMPHSi are present in plasma prepared PMPHSi. The presence and intensities of vibrations Si–C_{ar} (1110 and 1423 cm^{-1}) are not changed in all materials. Also other C–H bonding vibrations fingerprints present in solution polymer in $600\text{--}700 \text{ cm}^{-1}$ and $2900\text{--}3000 \text{ cm}^{-1}$ are preserved in the plasma prepared films. The most obvious change in plasma films compared to solution processed films is the existence of the more stable Si–CH₂–Si units ($1039\text{--}1050 \text{ cm}^{-1}$) and the existence of the carbidic units Si–C near 800 cm^{-1} and Si–H near

2100 cm^{-1} are visible both in MW and RF plasmatic films.

3.2. Optical and fluorescence properties

The plasma prepared PMPPhSi films display in many aspects very similar properties compared to solution processed films. The optical absorption and PL emission spectra of solution processed PMPPhSi [29] and typical RF plasma PMPPhSi film are in Fig. 9 a and b, respectively. In optical absorption of solution processed PMPPhSi (Fig. 9a-bold line), there is an exciton peak at 338 nm, the second absorption band at 276 nm occurs ($\pi-\pi^*$ transitions in the phenyl side groups) and the absorption peak at 195 nm (mainly $\pi-\pi^*$ transitions as it follows from quantum chemical calculations) [30]. The PL emission spectrum excited by 280 nm (dotted curve) shows the excitonic deactivation radiation ($\sigma^*-\sigma$) at 355 nm with a small Stokes shift of about 20 meV. The fluorescence quantum efficiency is quite high, about 0.15 at 355 nm. Fig. 9b shows the corresponding dependencies — absorption and PL spectra for the RF plasma PMPPhSi prepared under partial pressure of hydrogen 60 Pa and monomer 20 Pa, where the excitonic PL is observed situated at $\lambda = 320$ nm (Si $\sigma^*-\sigma$). Absorption exhibits the excitonic bands at 320 nm (Si $\sigma-\sigma^*$), 260 and 225 nm, and also a tail in long wavelength region typical for disordered materials.

We observed a strong wavelength excitation dependence of emission spectra in the PL spectra. It has been revealed that the structural defects of PMPPhSi, which consist not only of the branching points but also of defects, produced inevitably during the polymerization and material-ageing act as radiative recombination centers for the defect-like PL in the visible region in the wide region of 450–600 nm [31]. This is visible in detail for solution processed PMPPhSi in Fig. 10 a, where are the PL emission spectra for excitation wavelength 250, 300 and 350 nm. The differences indicate that the relaxation of the excited states is possible by several competitive processes. In Fig. 10 b this effect is depicted in some detail for the plasma PMPPhSi, where two PL

emission spectra are given for $\lambda = 210$ and 280 nm excitation wavelengths. The PL emission spectrum with the excitation wavelength 280 nm contains both the Si main chain $\sigma^*-\sigma$ exciton at $\lambda = 325$ nm and defect-like PL band (around 480 nm), whereas the excitation at 210 nm gives only excitonic PL.

The identification of both the excitonic and defect-like PL was confirmed by the time resolved PL measurements in Fig. 11. The strong excitonic 355 nm emission of the solution processed PMPPhSi decays approximately as a single exponential with the time constant $\tau_1 \leq 100$ ps. This lifetime is consistent with other measurements on other linear silicon chain polymers [14,32]. The temporal characteristics of the visible band near 450–500 nm are substantially different, the data are highly non exponential with decay times distributed over the interval 10^{-9} – 10^{-7} s (Fig. 11). The emission of the optimised samples (D3) RF plasma polymerised PMPPhSi is composed of the sharp excitonic emission around 360 nm as well as a broad visible PL emission. The former may be again attributed to excitons on a linear silicon chain with the lifetimes comparable to the decay times in a solution processed PMPPhSi film, whereas the latter exhibits two time constants 10^{-9} and 10^{-8} s.

The similarity of solution processed solid state PMPPhSi film and plasma produced polymer films is still more expressed for samples prepared under remote MW plasma under ECR regime (MW5: partial pressure of hydrogen 0.1 Pa, partial pressure of monomer 0.030 Pa, substrate temperature 90–100 °C). In Fig. 12 there are comparative PL emission spectra of both RF and MW plasma films with solution processed PMPPhSi film, showing similarity of PL emission spectra at about 360 nm of both materials and testifying the progress in the techniques of plasma preparation of nanostructural plasma PMPPhSi.

3.3. Degradation and metastability

It is well known that UV radiation in combination with oxygen and moisture influences many physical and

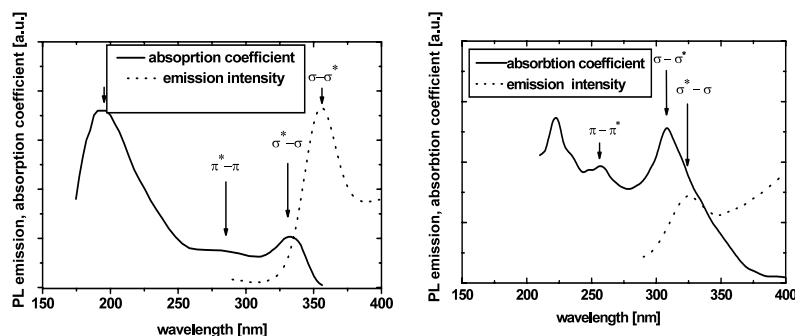


Fig. 9. Absorption and emission PL spectra of solution processed PMPPhSi (a), RF plasma prepared PMPPhSi (b); emission PL spectra excited at 280 nm.

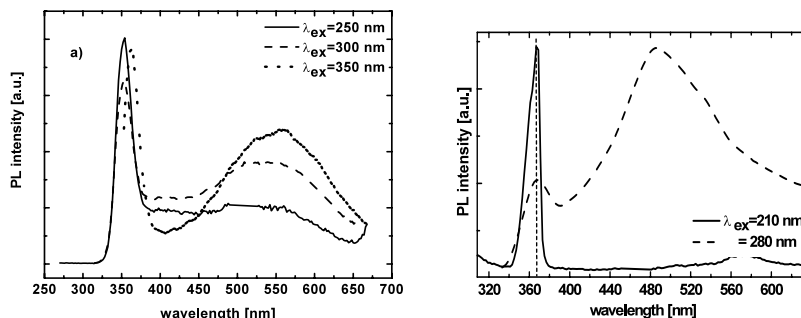


Fig. 10. Emission PL spectra of PMPHSi — solution processed (a) and RF plasma prepared (b), parameter is the excitation wavelength.

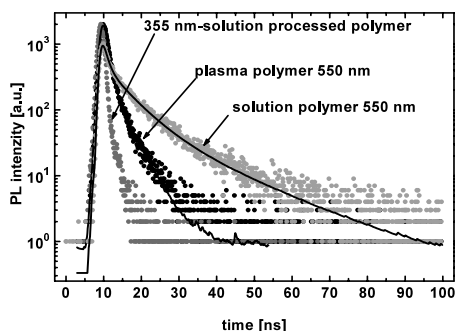


Fig. 11. Decay of the PL of solution processed and RF plasma prepared PMPHSi films.

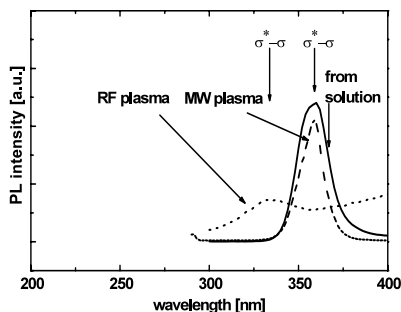


Fig. 12. Comparative PL emission spectra of solution processed PMPHSi, RF plasma polymerised PMPHSi (D3: 60 Pa hydrogen partial pressure, 20 Pa monomer partial pressure, 80 °C substrate temperature, and 1.4 W cm⁻² RF power density) and MW plasma polymerised PMPHSi (MW5: 0.1 Pa hydrogen partial pressure, 0.030 Pa monomer partial pressure, 90–100 °C substrate temperature).

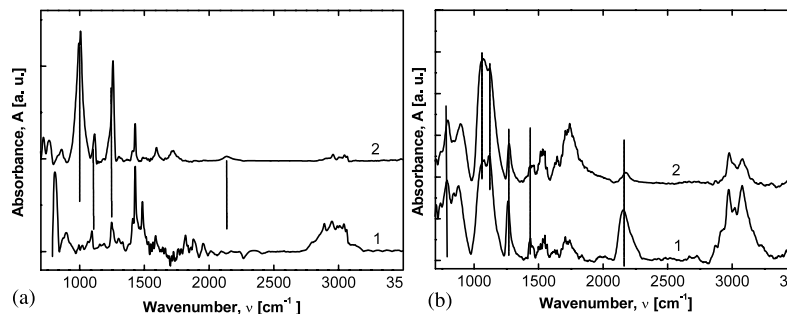


Fig. 13. IR spectra of solution processed (a) and RF plasma (b) prepared PMPHSi before (1) and after (2) degradation by 266 nm.

chemical properties of the polysilenes solid films [33]. In Fig. 13 are IR absorption spectra of PMPHSi prepared from solution (Fig. 13a) and in RF plasma (Fig. 13b) before and after degradation by UV radiation $\lambda = 266$ nm for 3600 s. The measurements are unique, as they are done using the IR microscope immediately after UV irradiation, so the oxygen reactions were suppressed to a great deal.

There is hardly any change in bonding of phenyl in both materials after degradation ($\text{Si}-\text{C}_{\text{ar}}$ at 1120 and 1427 cm^{-1}), but there are changes in bonding of aliphatic carbon $\text{Si}-\text{C}_{\text{ali}}$ (1046 and 1253 cm^{-1}). The most expressed change is the increase of the more stable $\text{Si}-\text{CH}_2-\text{Si}$ units in the solution processed and RF plasma prepared film (1039–1050 cm^{-1}) and the subsequent creation of carbidic units $\text{Si}-\text{C}$ near 800 cm^{-1} in both plasmatic materials. We explain the metastability of the PMPHSi by the creation of $\text{Si}-\text{CH}_2-\text{Si}$ and $\text{Si}-\text{H}$ bonds after degradation process [34].

The influence of thermal degradation on the optimised plasma PMPHSi as reflected on PL are in Figs. 14–16. In Fig. 14 there are desorption spectra with three species observed — that originating from phenyl C_6H_6 , methyl CH_3 and hydrogen H.

In Fig. 15 there are corresponding PL emission spectra excited by 280 nm after anneal to marked temperatures during measurements of desorption spectroscopy in Fig. 14. Both excitonic (355 nm) and defect-like (483 nm) PL is present in PL emission spectra of the virgin sample. After anneal the excitonic PL intensity slowly decreases, whereas the defect-like PL intensity in

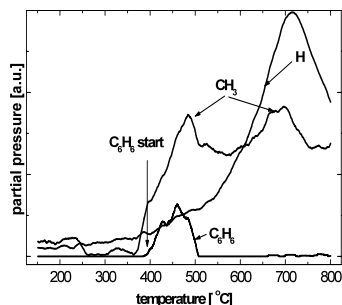


Fig. 14. The influence of the thermal degradation process on RF plasma PMPHSi, the desorption spectra (a), corresponding excitation PL spectra taken at 335 nm (b), (D3 sample).

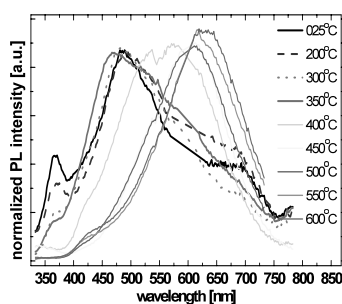


Fig. 15. The thermal degradation process in RF plasma PMPHSi — influence on PL emission spectra after anneal to marked temperatures corresponding to measurements in Fig. 14; excitation wavelength 280 nm.

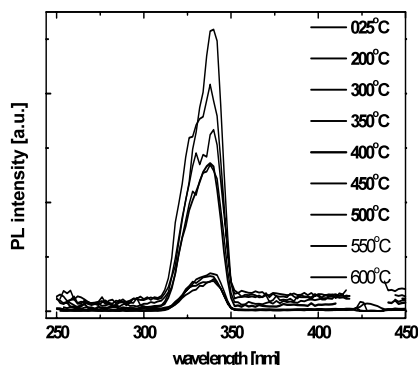


Fig. 16. The detail of the thermal degradation process in RF plasma PMPHSi — influence on PL emission spectra after anneal to marked temperatures corresponding to measurements in Fig. 14; excitation wavelength 213 nm.

not changed, but gradually shifted to longer wavelengths. At the temperature of 400 °C the excitonic PL is quenched and at higher temperatures of anneal the gradual shift of the visible PL to 620 nm occurs. It is worth to notice the correlation of these effects with the desorption of phenyl species in the temperature interval 390–506 °C. These conclusions are confirmed by the PL emission excited by 213 nm in Fig. 16, where the

excitonic PL is strongly correlated with the desorption of phenyl species.

4. Conclusions

The plasma polymers prepared from silicon monomers are materials with 1D silyl, 2D silene to 3D carbidic bonding. They may be prepared with controlled transition from one to other morphology, depending on the preparation conditions [22,23]. The microphysical properties and stability of the materials change accordingly and a wide range of materials may be prepared depending on the conditions of plasma polymerization. In the present study we aimed at the nanostructural silicon materials with combined 1D and 2D (3D) structure possessing excitonic PL, stability towards UV radiation and good charge-carrier transport properties.

We proved that RF plasma produced poly[methyl(phenyl)silylene] — PMPHSi under optimised conditions — the total gas pressure in a small range 80–90 Pa with the maximum possible of both hydrogen pressure of 60 Pa, monomer pressure in a small range 20–30 Pa and substrate temperature about 80 °C with the power density of about 1.5 W cm^{-2} — forms a nanostructural material with controlled 1D nanostructural islands of polysilylenes embedded in 3D amorphous network forming a cage effect, in some properties very similar to standard polysilylenes prepared from solution. Similar and better properties give MW plasma produced polysilylenes under conditions: 0.1 Pa H_2 , 0.030 Pa monomer, 90–100 °C substrate temperature. This conclusions were supported by the microphysical properties of films and their desorption spectra. We found the main indicator of the quality of the material as to PL and mechanical properties to be the highest possible temperature of all effused species in a thermal desorption spectrum, with minimum of phenyl peaks indicating ordered and stable structure of films. The resistivity of such optimised nanostructural materials to external UV radiation is greatly increased compared to polymers prepared from solutions.

Acknowledgements

This work was supported by Grant agency of the Czech Republic No. 202/01/0518.

References

- [1] R.D. Miller, J. Michl, Chem. Rev. 89 (1989) 1359.
- [2] L.A. Harrah, J.M. Zeigler, Macromolecules 20 (1987) 601.
- [3] Y. Nagai, H. Watanabe, H. Matsumoto, Y. Naoi, N. Sutou, Adv. Chem. Ser. 224 (1990) 505 (Chapter 27).

- [4] I. Kmínek, S. Nešpůrek, E. Brynda, J. Pflieger, V. Cimrová, W. Schnabel, *Collect. Czech. Chem. Commun.* 24 (1993) 2337.
- [5] I. Borthwick, L.C. Baldwin, M. Sulkes, M.J. Fink, *Organometallics* 19 (2000) 139.
- [6] N. Matsumoto, *Jpn J. Appl. Phys.* 37 (1998) 5425.
- [7] L. Brus, *J. Phys. Chem.* 98 (1994) 3575.
- [8] S. Hayase, *Chemtech* 24 (1994) 19.
- [9] M.A. Abkowitz, M. Stolka, *J. Non-Cryst. Solids* 114 (1988) 342.
- [10] E. Brynda, S. Nešpůrek, W. Schnabel, *Chem. Phys.* 175 (1993) 459.
- [11] F. Kajzar, J. Messier, C. Rosilio, *J. Appl. Phys.* 60 (1986) 3040.
- [12] S.-H. Jung, H.K. Kim, *J. Lumin.* 87–89 (2000) 51.
- [13] S. Ninomiya, Y. Ashihara, Y. Nakayama, K. Oka, R. West, *J. Appl. Phys.* 83 (1998) 3652.
- [14] W.L. Wilson, T.W. Weideman, *J. Phys. Chem.* 95 (1991) 4568.
- [15] A. Watanabe, Y. Tsutsumi, M. Matsuda, *Synthetic Met.* 74 (1995) 191.
- [16] M. Suzuki, Y. Nakata, H. Nagai, K. Goto, O. Nishimura, T. Okutani, *Mat. Sci. Eng. A* 246 (1998) 36.
- [17] A. Watanabe, T. Kawato, M. Matsuda, M. Fujitsuka, O. Ito, *Thin Solid Films* 312 (1998) 123.
- [18] H. Biederman, Y. Osada, *Plasma Polymerization Processes*, Elsevier, Amsterdam, 1992.
- [19] P.D. Buzzard, D.S. Soong, A.T. Bell, *J. Appl. Polym. Sci.* 27 (1982) 3965.
- [20] T. Nakamura, V.A. Sinegersky, T. Hirano, K. Fuki, H. Koinuma, *Macromol. Chem.* 189 (1988) 1315.
- [21] H. Nagai, Y. Nakata, M. Suzuki, T. Okutani, *J. Mater. Sci.* 33 (1998) 1897.
- [22] A.M. Wrobel, S. Wickramanayaka, Y. Nakanishi, Y. Fukuda, Y. Hatanaka, *Chem. Mater.* 7 (1995) 1403.
- [23] A.M. Wrobel, A. Walkiewicz-Pietrzykowska, *Chem. Mater.* 13 (2001) 1884.
- [24] Faculty of Chemistry, Brno University of Technology, Brno, Czech Republic.
- [25] V. Čech, P. Horváth, J. Jančář, F. Schauer, S. Nešpůrek, *Chem. Papers* 293 (1999) 165.
- [26] O. Salyk, A. Poruba, F. Schauer, *Chem. Papers* 50 (1996) 177.
- [27] D.R. Anderson, in: A.L. Smith (Ed.), *Analysis of Silicones* (Chapter 10), Wiley–Interscience, New York, 1974 (Chapter 10).
- [28] E.D. Lipp, A.L. Smith, in: A.L. Smith (Ed.), *The Analytical Chemistry of Silicones* (Chapter 11), Wiley–Interscience, New York, 1991 (Chapter 11).
- [29] K. Navrátil, J. Šik, J. Humlíček, S. Nešpůrek, *Opt. Mater.* 12 (1999) 105.
- [30] O. Itoh, M. Terazima, T. Azumi, N. Matsumoto, K. Takeda, M. Fujino, *Macromolecules* 22 (1989) 10718.
- [31] S. Nešpůrek, F. Schauer, A. Kadashchuk, *Chem. Monthly* 132 (2001) 159.
- [32] I.D.W. Samuel, B. Crystall, G. Rumbles, P.L. Burn, A.B. Holmes, R.H. Friend, *Synthetic Met.* 54 (1993) 281.
- [33] O. Meszároš, P. Schmidt, J. Pospíšil, S. Nešpůrek, *J. Polym. Sci., Poly. Chem. Ed.*, in press.
- [34] F. Schauer, N. Dokoupil, P. Horváth, I. Kuritka, S. Nešpůrek, *Macromol. Symp.*, in press.